Island Arc (2007) **16**, 224–242

Research Article

The Oka Belt (Southern Siberia and Northern Mongolia): A Neoproterozoic analog of the Japanese Shimanto Belt?

ALEXANDER KUZMICHEV,[1]* EVGENY SKLYAROV,[2] ANATOLY POSTNIKOV[3] AND ELENA BIBIKOVA[4]

[1]*Geological Institute of Russian Academy of Sciences, Pyzhevsky 7, 119017 Moscow, Russia (email: kuzmich@ilran.ru),* [2]*Institute of the Earth's Crust of Siberian Branch of Russian Academy of Sciences, Lermontova 128, Irkutsk, Russia,* [3]*Institute of Geology of Siberian Branch of Russian Academy of Sciences, Acad. Koptyuga 3, Novosibirsk, Russia and* [4]*Vernadsky Institute of Geochemistry and Analytical Chemistry, Russian Academy of Science, Kosygina Str. 19, Moscow, Russia*

Abstract The Oka Belt, composed of clastic rocks and greenschists, extends for approximately 600 km in the South-Siberian Sayan region and adjacent northern Mongolia. For a long time the Oka Belt's age and tectonic setting were the most controversial problem in the region. We argue that the belt was formed in Late Neoproterozoic as an accretionary prism. The Oka Belt shows imbricated thrust structure, which had originally seaward vergence and reflected the Neoproterozoic accretion process. The Early Paleozoic orogeny had minor effect on its structural style. The belt contains tectonic slivers of mid-ocean ridge basalts, some oceanic-island basalts and possible pelagic sediments. In several localities they are associated with gabbro and serpentinite. All these rocks represent the oceanic lithosphere subducting beneath the Oka prism and trapped within it. In the inner zone of the Oka Belt are the blueschists exhumed from the deeper prism level. The northern Oka Belt includes mafic intrusions geochemically similar to normal mid-oceanic ridge basalt and felsic volcaniclastic rocks. This segment of the belt is very similar to the Tertiary portion of northern Shimanto Belt, in Japan, and has also experienced the subduction of orthogonal oceanic ridge beneath the prism. This event dates back to 753 ± 16 Ma (the U-Pb zircon discordia). The Oka prism started accreting in Mid-Neoproterozoic after the subduction had initiated under the Japan-like South-Siberian continental terrain. The prism existed through the second half of Neoproterozoic and accumulated a huge volume of sialic material to enlarge the nearby continent. Currently, the Oka Belt remains poorly studied and is very promising for further investigation and discoveries.

Key words: accretionary prism, blueschists, Central-Asian Fold Belt, Mongolia, Neoproterozoic tectonics, Sayan, Siberia.

INTRODUCTION

The Neoproterozoic Oka Belt composed of clastic rocks and greenschists occupies the area of approximately 8000 km^2 on the territory of Southern Siberia and Northern Mongolia (Fig. 1). This is a major tectonic feature of the region, and clarification of its origin is important for recognition of Late Precambrian evolution of the Central Asian Fold Belt. Yet, the Oka Belt has not been studied properly, probably for two reasons. First, the ancient accretionary prisms are not so notable and attractive geological objects as the surrounding ophiolites and island-arc complexes, which could be easily identified and dated. Geological mapping and isotopic dating of the Oka Belt is difficult because of the complicated structure and monotonous rock composition. The second reason is our poor knowledge on the geology of modern accretionary prisms, which was common for most of

*Correspondence.

Received 10 January 2006; accepted for publication 7 November 2006.

doi:10.1111/j.1440-1738.2007.00568.x

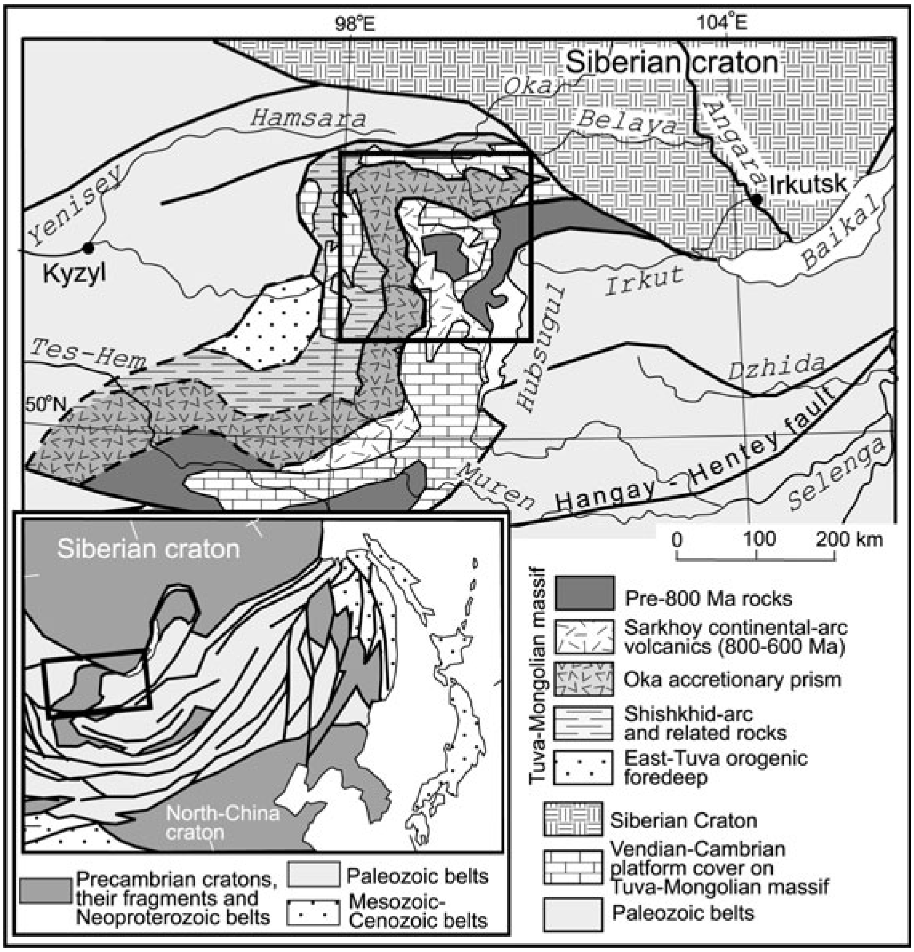

Fig. 1 Late Neoproterozoic zonality of Tuva-Mongolian Massif. The box shows outline of Figure 2 in the inlet – position of the Tuva-Mongolian massif (in the box) in the East-Asian tectonic framework.

Russian Precambrian geologists in the 1970s and 1980s, when extensive geological surveys were carried out in Siberia and Mongolia.

During the entire span of regional geological surveys, the geologists faced the problem of adequate description of the Oka Belt. Numerous versions were suggested for its age and stratigraphic subdivision and all of them were quite contradictory (Arsentiev & Volkolakov 1964; Dodin *et al.* 1971; Katyukha & Rogachev 1983; Roschektaev *et al.* 1983; Kuzmichev 1997). The routine stratigraphic methods used by most of the above authors turned to be inapplicable for such terrains as the Oka Belt. More reasonable was the viewpoint by Postnikov and Sklyarov 1988 and Belichenko *et al.* 1989, who described the Oka Belt as a combination of three units of different age and origin. However, it is quite impossible to get an adequate impression of what the Oka Belt is like, and what its age is on the grounds of available publications.

We studied the Oka Belt in the 1980s and 1990s, and the current study provides reinterpretation of our former field data, using the Shimanto Belt and other young accretionary complexes as standard ones. Our field observations were insufficient to describe in detail all aspects of the Oka Belt geology in the context of accretion analysis. Nevertheless, we believe that systematic compilation of the data allows proving that the Oka Belt is really a fossil accretionary prism.

The main goals of the present study are as follows. (i) To provide arguments for the accretionary prism origin of the Oka Belt. This interpretation is important for understanding Neoproterozoic paleogeography and allows to combine the known Late Neoproterozoic features of the Central Asian Fold Belt into a coherent geodynamic context. (ii) To stimulate the studies of some Neoproterozoic 'turbidite terrains', which can be interpreted as possible accretionary prism fragments. We suggest that the terrains similar to the Oka Belt are widespread around the Siberian platform but remain unrecognized. (iii) To draw attention to this remarkable geological object, which is still not studied adequately. We particularly wish to attract attention of Japanese geologists skilled in the accretion analysis, because almost all the Japanese Islands are composed of Late Paleozoic to Tertiary accretionary complexes (e.g. Taira *et al.* 1988).

GENERAL GEOLOGICAL SETTING

The Oka Belt comprises a part of the Tuva-Mongolian Massif – one of Precambrian terrains, located in the Central Asian Fold Belt (Fig. 1). The Tuva-Mongolian Massif is predominantly composed of Neoproterozoic rocks, unconformably covered by Vendian-Cambrian shallow-water carbonate deposits. They were folded and thrust faulted as a result of Early Ordovician orogeny and presently do not look like a platformal cover. Yet this carbonate complex is a distinguishing feature of the massif, because the rocks of the same age are represented by the island-arc volcanics and terrigenous deposits in the surrounding regions.

The Tuva-Mongolian Massif shows a distinct Neoproterozoic zonality. The Oka Belt extends between the two Late Neoproterozoic terrains: the Sarkhoi continental arc to the ESE and the Shishkhid oceanic island arc to the WNW (Fig. 1). The first terrain is an ancient continental block, which presumably formed the edge of the Precambrian Siberian continent. It was affected by collision with an island arc in the Mid-Neoproterozoic time (Kuzmichev *et al.* 2001). After this event, a subduction of oceanic plate initiated under the continent, and the Late Neoproterozoic Sarkhoi Volcanic Belt, composed mostly of ignimbrite, arose on this basement (Kuzmichev 2004). We believe that the Oka Belt is an ancient accretionary prism that has formed along this continental margin. On the other side of the Oka Belt lies the terrain that we attributed to the Shishkhid Island Arc. It lacked the Early Precambrian basement (as was earlier believed) and was built up during the Late Neoproterozoic (Kuzmichev *et al.* 2005). The rear side of the Shishkhid Arc was oriented in the direction of the Oka prism. All these three elements of the Late Neoproterozoic paleogeography have ceased in the course of collision of the Shishkhid and Sarkhoi Arcs, which occurred at the end of Neoproterozoic (Kuzmichev *et al.* 2005).

The Oka Belt is fringed by thrust zones on both sides, dipping eastward or northward. They are the distinct major faults in the northern Oka Belt. In its southeastern part, composed of metamorphic rocks, these borders can be traced only presumably. The thrusts were formed at the end of Neoproterozoic (Kuzmichev *et al.* 2005) and reactivated in the Early Ordovician time. Vendian and Cambrian carbonate rocks, which formerly represented platformal cover of the Tuva-Mongolian Massif, were also involved in the thrusting (Fig. 2).

The rocks forming the studied northern portion of the Oka Belt were designated as the Oka Group in the Russian territory, whereas in Mongolia they were named the Khugein Group. The belt is not homogenous in composition. First, two metamorphic blocks (Kharatologoy and Shutkhulay, Fig. 2) made up with amphibolite-facies rocks stand out. They were formerly interpreted as salients of Early Precambrian basement, but are now treated as metamorphosed Oka Group (Aktanov & Sklyarov 1990; Donskaya *et al.* 2004).

As we believe that in Late Neoproterozoic the Oka prism accreted in front of the Sarkhoi Continental Arc, we hereafter designate the direction toward it (ESE) as 'landward', and the opposite direction toward the Shishkhid Arc (WNW), which in Late Neoproterozoic was separated from the Oka prism by an ocean, is then termed 'seaward'.

STRUCTURE OF THE OKA BELT

The deformations are not uniform throughout the Oka Belt, which contains both strongly deformed mélange zones and more coherent blocks. The style of deformation also depends on the degree of metamorphic alteration caused by the Ordovician orogeny that was responsible for emplacement of numerous granite plutons (Fig. 2). Clastic rocks of the Oka Group show synkinematic dynamic recrystallization even in the biotite zone, which might have caused the development of a newly formed synmetamorphic structure (Fig. 3). Thus this chapter mainly deals with the least altered rocks exposed in the Yakhoshop and Dayalyk River Basins (Fig. 4).

In this area, the Oka Belt falls into numerous slivers separated by sublatitudinal high-angle faults dipping northwards. As a result of poor exposure we could map only major faults separating different lithologies. They are oriented in accordance with overall southward vergence typical of this segment of the Oka Belt. This vergence was mainly due to Early Paleozoic orogeny, which occurred long after the Oka prism had formed. We suggest that this fault system was originally inclined southwards and had 'seaward' vergence, typical of accretionary prisms. Some features sup-

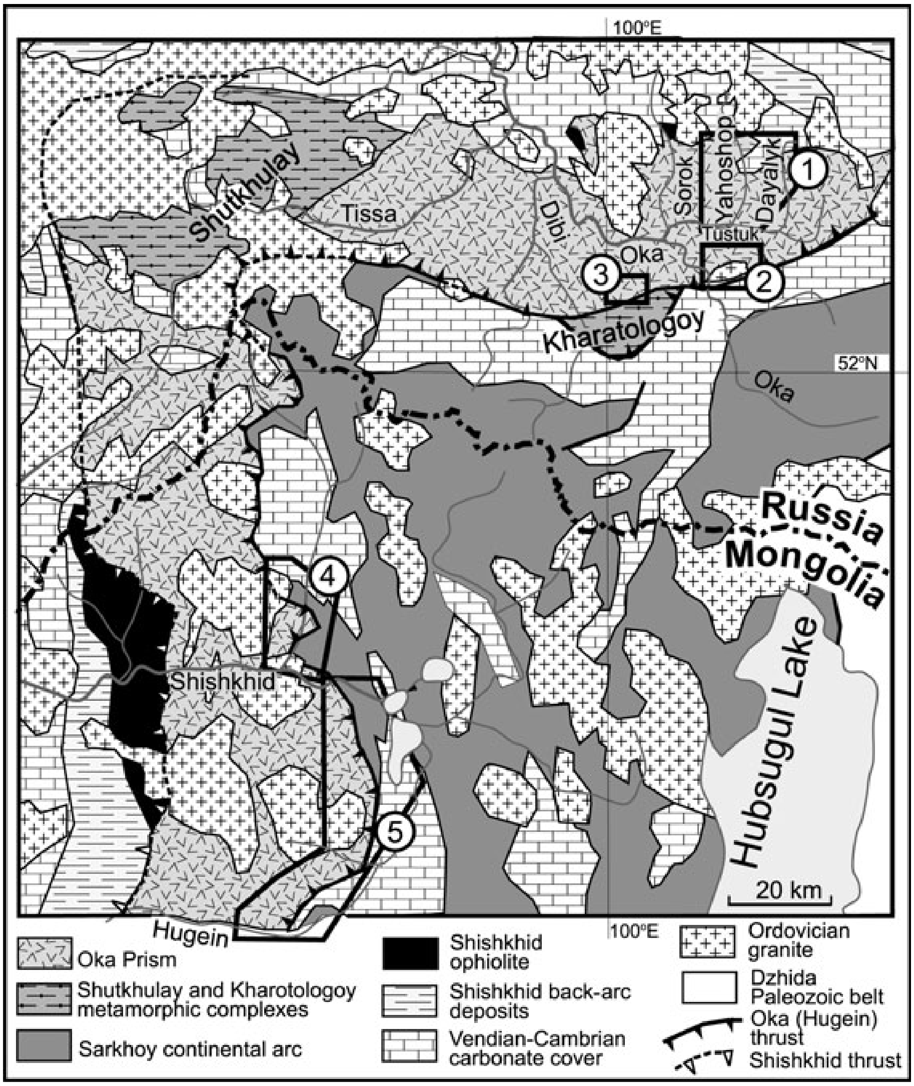

Fig. 2 Geological map of the northern Oka Belt. Areas mentioned in the text are outlined: (1) Yakhoshop and Dayalyk (Fig. 4); (2) Haigas; (3) Hazalkhy; (4) Tengesin; (5) Hugein (Fig. 6).

Fig. 3 Ductile deformation of metamorphosed (biotite zone) sandstone-shale alternation. Although the rock could be deformed in non-lithified conditions in Neoproterozoic, we cannot exclude structural overprinting as a result of Ordovician synmetamorphic shear strain. Sample 765/1, Haigas area (Fig. 2). The image width is 23.3 mm.

porting this idea can be found in the Dashtag and Dayalyk River Basins (Fig. 4). First, the observation of grading and cross-bedding in turbidite sediments indicates that in all recorded cases the layers' tops were faced southwards. In particular, the Oka Group strata on the well-exposed left slope of the Dashtag River dip steeply northwest, which is nearly parallel to the faults, and show the overturned position. It is very likely that in the Neoproterozoic time these strata were in normal position and were inclined southeast as well as the thrust sheets. Second, orientation of some drag folds is inconsistent with the recent southward vergence and might indicate original northward thrusting (Fig. 5a).

Some major faults can probably be unrelated with accretion processes and are younger in age. For example, the main latitudinal fault in the center of the mapped area (Fig. 4) divides the area

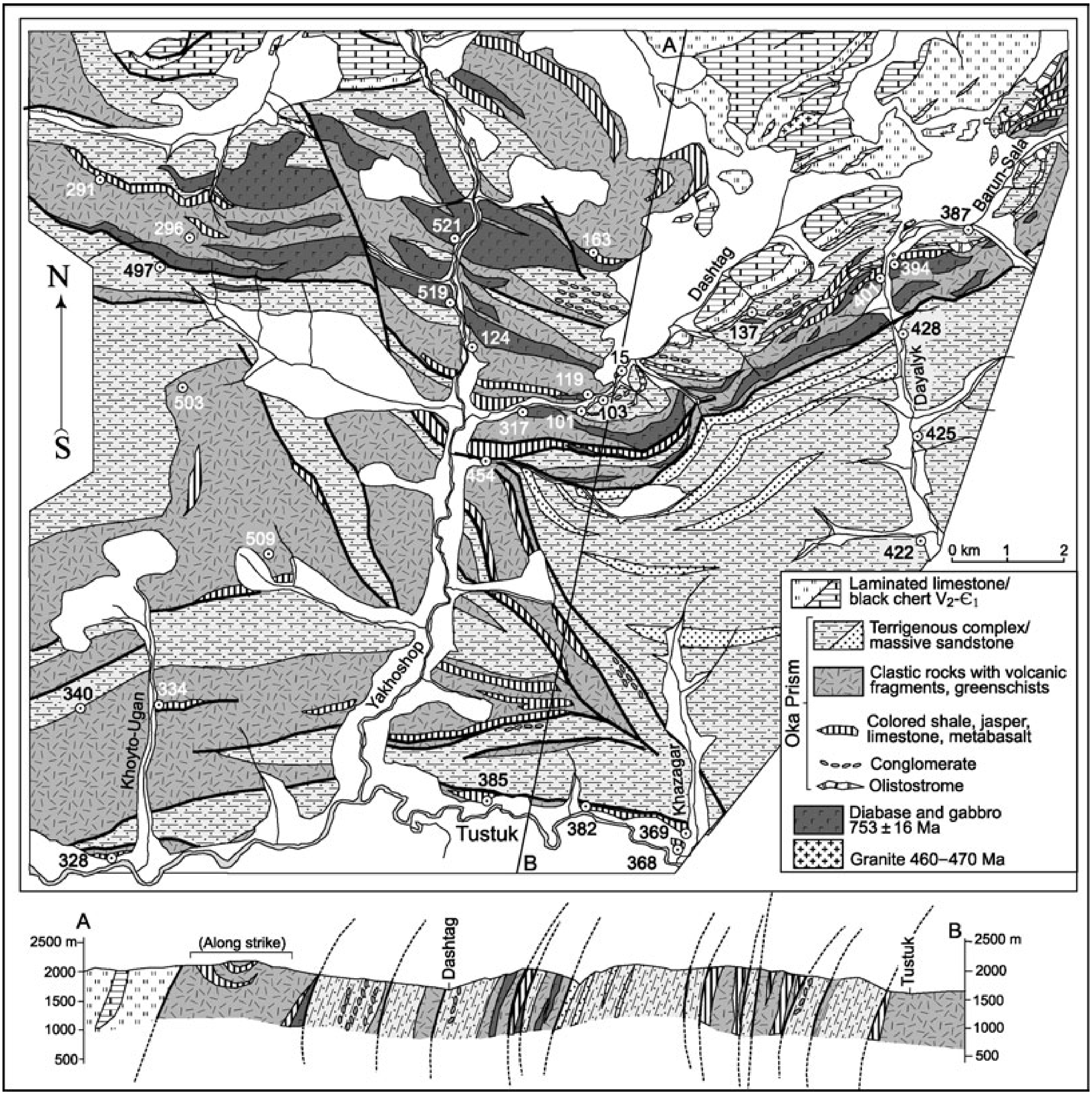

Fig. 4 Geological map of Yakhoshop and Dayalyk area; see Figure 2 for location. Shown site numbers mentioned in the text and figures.

into two parts differing in rock composition, which might indicate significant displacement. The northern block contains less volcaniclastic rocks and lacks olistostrome. The diagonal discordant faults, which can be seen in Figures 4 and 6 are Ordovician in age (Kuzmichev 2004).

Coherent flysch packages with planar bedding are rare in the area shown in Figure 4, although to the west and southwest they are more common. In the studied area, the majority of terrigenous rocks have primarily been deformed in soft or semilithified conditions (Fig. 5a,b). Quite typical is fragmentation of sandstone layers, caused by shearing, which can be attributed to underthrusting process. Such structure occurs either in microscopic (Fig. 7d,e), hand specimen, or outcrop scale (Fig. 5a). This disturbed layering is responsible for specific rock appearance in the exposures: they rarely produce slate-like or slab-like debris, but usually occur in the form of irregular blocks because of irregular inner structure.

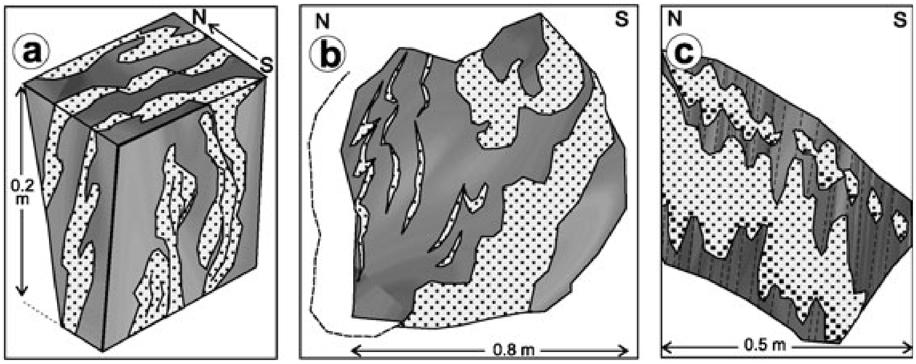

Fig. 5 Field drawings of some structural features of Oka Group on the banks of Dayalyk River. The site numbers are shown in Figure 4. (a) Complex boudinage of sandstone layers (site 425). Drag folds are inconsistent with recent southward vergence and might indicate the earlier northward ('seaward') thrusting. (b) Complex deformation of fold hinge occurred in soft conditions (site 422). (c) Layer parallel compression, which caused schistosity (dips northward at 80°). It follows the previous stage stretching, which caused necking of sandstone layers (dips southward at 30–40°, normal position). Site 428.

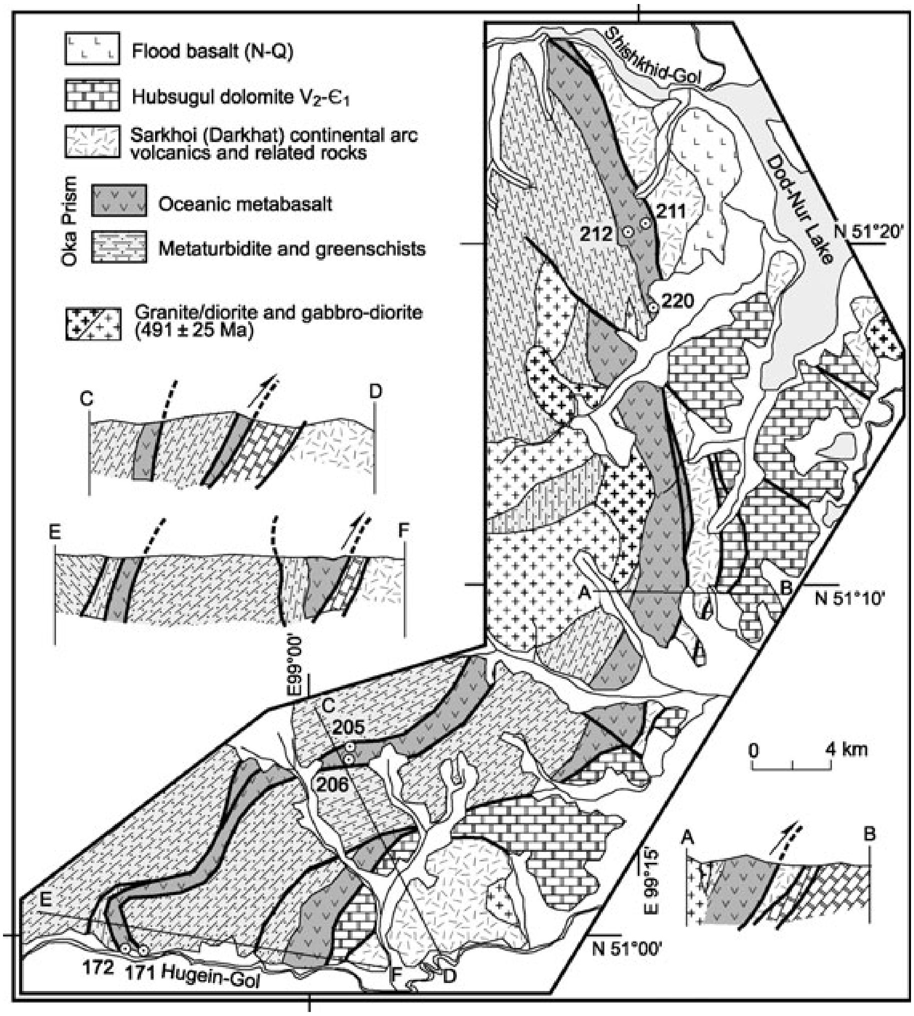

Fig. 6 Geological map of Hugein area; see Figure 2 for location. The mentioned site numbers are indicated.

One of the earliest structural features is the layer-parallel extension, which is expressed by stretched and boudinaged layers. The majority of rocks show strong layer-parallel extension, which in most cases is overprinted by the second-stage compressional deformations. Boudinage of sandstone layers is quite common for clastic rocks. Elongation of boudins is not always horizontal. There occurred steeply inclined sausage-like rotated boudins that may indicate strike slip displacement. The rock flattening is most evident in conglomerates (Fig. 7a,b). Hard jasper or porphyry pebbles preserved their rounded shape, whereas shale pebbles were stretched sometimes to a high aspect ratio.

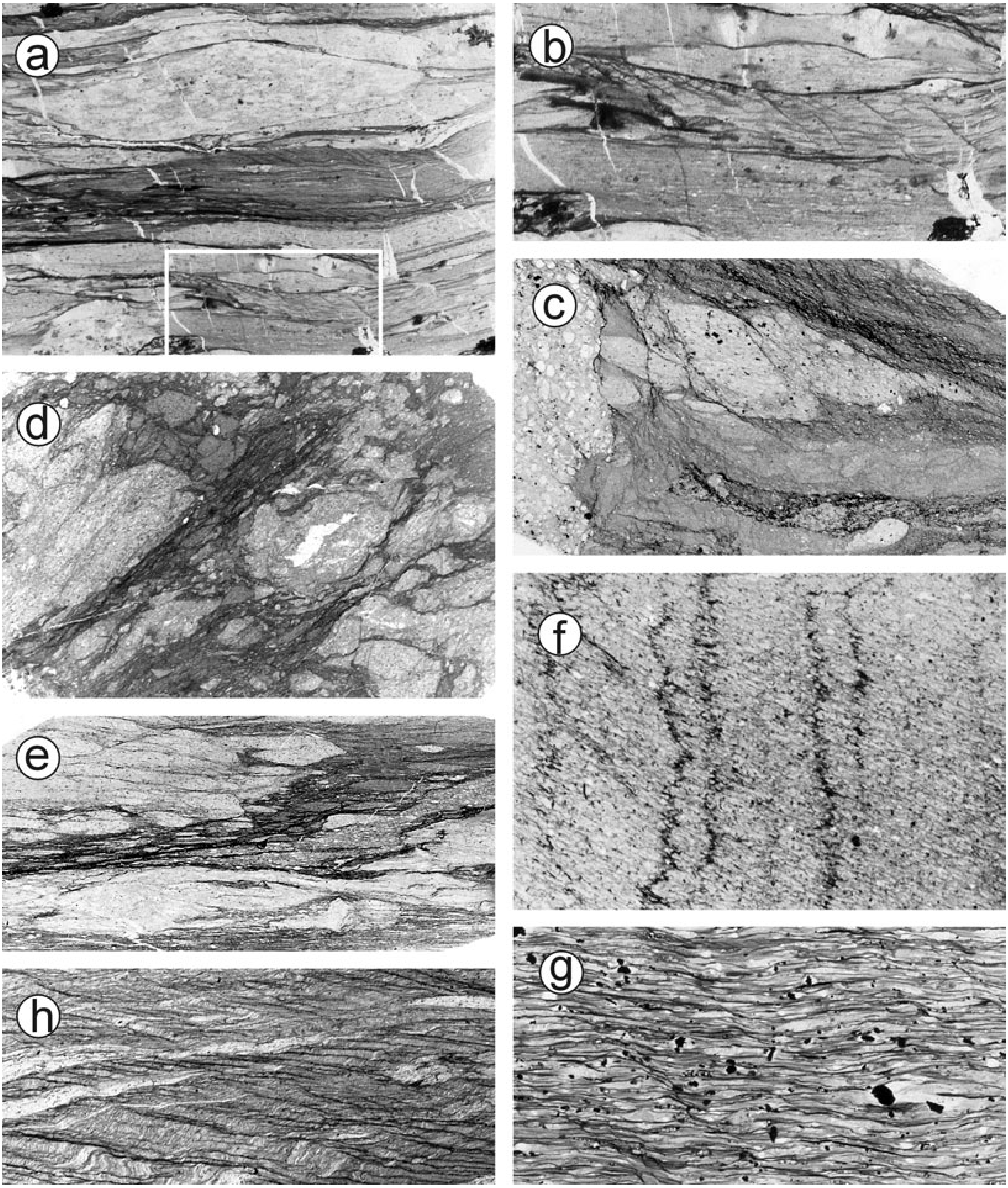

Fig. 7 The scanned thin section images to show the structural features of the Oka Group clastic rocks. The sample numbers correspond to site numbers in Figure 4. (a) Highly stretched flat-pebble shale conglomerate. Sample 103/1–93, 17.2 mm wide. Contour of image 'b' is outlined. (b) Fragment of the same thin section, showing strong flattening and incipient cleavage development in the matrix at a high angle. Width is 6.8 mm (c) Layer-parallel shortening is seen by the imbrication of previously flattened pebble fragments. Sample 387/2 – sandstone conglomerate with poorly sorted matrix. Image is 18.4 mm wide. (d) Fragmented sandstone layers in sandy mudstone matrix. The sample is cut normal to intersection lineation. Sample 509/1–94. The width is 17.6 mm (e) The same sample is cut along the intersection lineation. The image width is 21.1 mm (f) Shortening of layered siltstone as a result of along-layer compression and development of cleavage. Sample 497/1–94. Width is 10.8 mm (g) Incipient crenulation cleavage in schist. Dark grains are pyrite framboids fringed by pressure-shadow mineralization on both sides. Sample 137/2–93. Width is 14.2 mm (h) Further stage of crenulation cleavage development. Sample 101/1–93. Width is 9.7 mm.

Cleavage is common in the rocks of the northern Oka Belt. Usually, it looks like schistosity: irregular cleavage planes do not cut quartz grains in mudstone and could be formed in the incompletely lithified rocks. Quite often the schistosity is inclined at a high angle to bedding and indicates compression oriented almost opposite to primary layer-parallel extension (Figs 5c,7c,f). In accretionary complexes such compressional strain was attributed to underplating processes synchronous with the development of seaward thrusts and duplexes (Fisher & Byrne 1987; Sample & Moore 1987).

The next stage is the development of asymmetric crenulation cleavage (Fig. 7g,h), which usually occurred in the previously foliated rocks (Ramsey & Huber 1987). In the Oka Belt it has really affected the shales showing a large degree of previous layer-parallel extension, which is evident on pressure shadows by pyrite framboids (Fig. 7g). Caledonian orogeny might also take part in cleavage formation but we cannot confidently separate the two events. Its effect was obvious only in the lower reaches of the Dashtag River (site 15, Fig. 4), where two cleavage systems were observed cutting the rocks in rhombic fragments.

Although detailed structural observations which could indicate successive stages of deformation were not conducted in the field, the available data and examples provided by Figures 5 and 7 suggest the presence of accretionary prism.

THE OCEANIC ROCKS

A significant portion of the Oka Belt is represented by greenschists and amphibolites, which we attributed to metamorphosed ocean floor basalt and tuff. At several localities these rocks occur together with gabbro and serpentinite blocks and form dismembered ophiolite association. The northern Oka Belt contains jasper and red shale, which could probably be the oceanic sediments. We interpret all the above rocks as fragments of Late Neoproterozoic oceanic lithosphere trapped in the Oka accretionary prism.

OCEAN FLOOR BASALTS

Lenses and tectonic slivers of metamorphosed basaltic rocks can be found at any part of the Oka Belt, but they are more abundant in its inner part adjacent to the continental arc. For example, the northern limb of the Oka Belt (Fig. 4) contains rare metabasalts (e.g. site 454). They are presumably confined to the soles of thrust sheets and have turned into actinolite-chlorite-epidote schist. Southwards, their thickness increases. On the Tustuk River banks there appear slivers up to several tens of metres thick (sites 328, 385, Fig. 4). More southward, in the Haigas area (Fig. 3) thickness of the greenschist strata amounts to 800 m.

The best occurrence of oceanic basalts, including both the mid-oceanic ridge basalt (MORB)- and oceanic island basalt (OIB)-like varieties, is the Hugein River Basin (Fig. 6) (Sklyarov *et al.* 1996). In this section basalts compose the lowermost portion of the Hugein Group thrusted on the Sarkhoi continental-arc terrain. Total thickness of metabasalts is approximately 1000 m, although the section can be imbricated by minor thrusts. The rocks have generally lost their igneous textures and altered into epidote-chlorite-albite schist. The pillow structure has occasionally been preserved on the left bank of the Hugein River and is clearly visible near the contact with Hugein dolomites (Fig. 6). Sometimes the rocks show relics of ophitic or gabbro-ophitic texture, thus indicating the occurrence of intrusions along with erupted basalt. The dominating chlorite schists in the upper part of the section have been interpreted as metatuffs. Their primary clastic structure was observed only at Hugein River where they look like hyaloclastic breccia.

Metabasalts show homogenous chemical composition and are classified as tholeiitic basalts with moderate titanium (1.2–1.5% TiO_2) and iron (12–14% FeO) contents, and low alumina and potassium contents (Table 1). These features as well as Ti-V and Ti-Zr relationships indicate that the rocks could be attributed to MORB. At the distance of several kilometers northwest there is the next basaltic-picritic member (Fig. 6), which contains varieties with high concentrations of titanium (up to 4%), niobium (up to 83 ppm) and zirconium (up to 340 ppm) (Table 1). Such incompatible element enrichment might indicate an oceanic-island origin setting for these rocks.

Metabasalts were also analyzed at the Hazalkhy area (Fig. 2), where they share a similar composition with the Hugein MORB-like rocks (Sklyarov *et al.* 1996).

METAGABBRO AND ULTRAMAFIC ROCKS

Metagabbro, serpentinite and tremolite rock make up lenses and blocks, enclosed in the greenschist matrix. We have encountered such mélange in

Table 1 Chemical composition for mafic rocks in the Hugein area

Sample					Sole part of Oka belt								Inner part of Oka belt			
#	211b	211v	211g	211d	212a	212b	212v	212g	220a	205b	205d	206a	206b	206g	172a	171e
SiO_2	46.10	47.20	48.00	48.00	47.60	49.00	48.30	46.40	46.50	47.30	48.50	45.00	48.83	45.80	44.70	44.00
TiO_2	1.17	1.29	1.30	1.59	1.25	1.27	1.26	1.17	1.45	1.98	1.73	1.69	1.10	1.66	2.00	4.10
Al_2O_3	14.30	12.12	12.87	13.00	13.20	12.22	12.27	11.87	14.52	13.50	12.86	13.85	15.30	14.00	12.25	16.10
Fe_2O_3	5.06	6.92	7.47	5.72	6.93	7.75	6.83	8.76	3.69	0.12	3.21	4.69	3.59	6.01	1.51	4.06
FeO	7.86	8.38	6.53	7.65	6.38	5.56	5.92	6.02	10.42	13.99	8.26	7.96	7.34	8.38	11.74	9.19
MnO	0.17	0.17	0.17	0.14	0.14	0.14	0.17	0.14	0.19	0.19	0.19	0.17	0.17	0.17	0.23	0.23
MgO	8.22	5.95	5.88	7.13	6.37	6.55	6.55	5.90	6.66	7.45	8.63	11.05	7.76	7.38	12.76	6.57
CaO	8.04	8.86	9.33	8.96	11.07	9.29	10.02	9.29	10.17	9.89	9.89	8.84	9.64	9.91	8.91	8.60
Na_2O	3.16	3.49	3.59	3.04	2.09	2.91	2.98	3.04	2.57	2.94	2.18	2.17	3.16	2.91	0.80	3.15
K_2O	0.05	0.10	0.16	0.16	0.13	0.25	0.12	0.10	0.13	0.05	0.27	0.04	0.05	0.05	0.10	0.06
P_2O_5	0.09	0.19	0.12	0.15	0.12	0.16	0.09	0.12	0.27	0.16	0.18	0.14	0.08	0.14	0.18	0.60
LOI	5.57	5.53	4.91	4.45	4.58	4.90	4.98	6.59	3.13	2.58	4.01	4.68	3.12	3.59	5.16	3.21
Total	99.79	100.20	100.33	99.99	99.86	100.00	99.49	99.4	100.00	100.15	99.91	100.28	100.14	100.00	100.34	99.87
Rb	<4	<4	<4	<4	<4	5.1	5	<4	<4	<4	7	5	<4	<4	<4	<4
Sr	120	99	72	90	140	95	130	86	240	230	200	180	180	170	88	860
Ba	70	110	110	80	130	160	140	170	180	280	100	120	120	110	130	100
Cr	370	620	560	440	490	110	610	330	390	180	720	300	320	250	860	370
Ni	120	110	120	120	140	86	140	110	110	96	250	140	130	130	480	53
V	280	300	280	280	330	300	280	280	280	100	190	290	230	330	230	260
Y	24	25	29	28	24	27	25	30	29	32	24	25	21	29	19	33
Zr	69	69	100	70	66	74	66	70	80	96	108	103	62	100	125	340
Nb	6	<3	10	<3	<3	<3	<3	5	4	5	15	9	6	10	18	83

Analyses were made at the Geological Institute of Siberian branch of Russian Ac. Sci. (Ulan-Ude). Major elements were determined by classical chemical technique, trace elements with X-ray fluorescence spectrometry technique. Oxides in wt%, trace elements in ppm. Sample numbers correspond to site numbers in Figure 6. LOI, loss-on-ignition.

Haigas and Hazalkhy areas (Fig. 3), where they are associated with high-pressure metamorphic rocks. These exotic rocks form a specific dismembered ophiolitic association with the above basalts. The geochemistry of gabbroic rocks was poorly studied, although the available data show no island-arc affinity. So we suggest that the association represents the oceanic lithosphere.

OCEANIC SEDIMENTS

It was only in the northern Tustuk River Basin that some deposits could be presumably attributed to pelagic sediments. On the map (Fig. 4) they are shown by a general symbol of colored rocks, which embraces variegated mudstone, jasper and associated limestone. Thin-laminated colored (mostly reddish) and sometimes black argillite might represent a pelagic ooze. Such rocks have preserved initial sedimentary features around the site 163 (Fig. 4) and to a lesser degree on the Tustuk River northern bank (site 368, Fig. 4). In other outcrops, they have turned into variegated lustrous sericitic schists.

Jasper forms occasional massive, usually variously colored layers, up to several meters thick. At sites 454, 368 and 385 (Fig. 4) they are associated with metabasaltic greenschists and the above variegated shale and might represent pelagic cherts. However, the typical ribbon packages, so common for Mesozoic radiolarian cherts, are missing from the section. On the northern slope of the Tustuk Valley near the mouth of Khasagar Creek (site 368, Fig. 4), jasper accompanies hematite-rich rock containing up to 8% MnO (X-ray fluorescence spectrometry analysis), which can be attributed to oceanic metal-rich sediment. Some quartzose rocks were also reported in the Hugein and Hazalkhy sites (Belichenko *et al.* 1989; Sklyarov *et al.* 1996). They occur in combination with oceanic metabasalts and might have originated after cherts.

The assemblage of variegated argillites and jaspers in the Tustuk River Basin also contained limestone lenses up to several meters thick. They were recrystallized and did not preserve the primary lithology.

CLASTIC ROCKS

The Oka Belt is mainly composed of clastic rocks, which have usually lost their primary depositional structure. They are least altered in the belt's northern part. In this area, two groups of clastic rocks can be separately mapped. These are terrigenous rocks and clastic rocks with high contents of volcanic fragments. We presumably interpret both as slope and near-trench sediments. We have also described the olistostrome horizon, which probably underlies the isolated stratigraphic member.

TERRIGENOUS CLASTIC ROCKS

In the Tustuk River Basin (Fig. 4), the terrigenous complex is composed of irregular intercalation of shales and fine-grained sandstones including distinct layers of massive sandstones. The rocks are relatively well exposed on the banks of Dayalyk River. We have interpreted most of the Oka terrigenous rocks as turbidites although rhythmical flysch intercalation is rare.

Prevalent sediments are laminated or massive gray mudstones alternating with siltstones and fine-grained sandstones. Sandstone layers sometimes show basal erosion and normal grading, indicating a turbidite origin and allowing to determine the foot and top of the beds. However, the available observations are insufficient for logging of any significant part of stratigraphic section as a result of faulting and poor exposure. Certain layers show slump folds, convolute lamination and other features of soft-sediment deformation.

Massive sandstones form homogenous layers, up to several meters thick, which we interpret as the grain flow deposits. They show erosion at the foot and sometimes indistinct gradation. In their lower part there occur mudstone rip-up clasts. The upper part shows planar lamination. Sandstones are of greywacke composition and contain sedimentary and volcanic rock fragments, plagioclase and rounded transparent quartz grains.

Some sections also contain conglomerates with both platy shale fragments and medium- to well-rounded pebbles of hard rocks. Among them we identified jasper, sandstone, felsite, andesite, quartz porphyry, diorite, granophyre and tuff. Some well-rounded hard-rock pebbles were probably primarily processed on land.

VOLCANICLASTICS

Clastic rocks with bigger or lesser amount of volcanic fragments make up a significant volume of the northern outer zone of the Oka Belt. The most noticeable variety is the breccia composed of chaotically oriented angular igneous clasts up to 5 cm in size. Bigger fragments are represented by dacite (usually predominant), andesite, altered basalt and shale. Prevalent felsic clasts are plagioclase porphyry, quartz porphyry, granophyre and recrystallized felsites. Large feldspar and quartz grains are common in the matrix; they are fragments of granite and acid tuff. Detrital epidote is the product of metabasite destruction. Some breccias show rather homogeneous composition and look like tuffs. There are also medium- to fine-grained essentially volcaniclastic rocks.

The volcanic detritus could be derived from the neighboring Sarkhoi continental margin, which hosted the active volcanic belt at the same time as the Oka prism accumulated (Kuzmichev 2004). The granite and metamorphic rock fragments could result from continental basement erosion. However, some varietes do not show signs of long-distance transport and can be related with nearby volcanoes.

Chemical composition of the tuff-resembling volcaniclastic rocks corresponds to moderate- and low-K calk-alkaline dacites, enriched with light rare earth elements ($La_n/Yb_n = 8–11$, Table 2). The negative ε_{Nd} and Mesoproterozoic Nd model age (Table 3) are probably the result of contamination by ancient continental crust inherited from the Sarkhoi magmas.

OLISTOSTROME

The carbonate olistostrome is exposed in the Dashtag and Dayalyk River Basins (Fig. 4). It shows a changing lithology including large (up to several 100 m long and 20 m thick) olistoliths of massive or brecciated dolostones, fragments of carbonate beds twisted before lithification, carbonate breccia with angular fragments, as well as conglomerate with well-rounded boulders (up to 0.5 m) composed of limestones and dolostones of any sort. The clastic material includes fragments of both pliable and hard carbonate rocks. The former were probably deposited in a nearby carbonate shoal. Well-rounded boulders were first reworked on land and later transported downslope. The olistostrome horizon was also observed in other parts of the Northern Oka Belt (Katyukha & Rogachev 1983). This member is overlain by shale and sandstone intercalation, similar to the above mentioned terrigenous rocks. We could not elucidate if this member lay inside the regular Oka prism section or originally covered it unconformably.

BLUESCHISTS

A narrow zone including the high pressure–low temperature (HP–LT) metamorphic rocks was

Table 2 Chemical composition for volcaniclastic tuff-resembling rocks of Oka Group

	454/3	296/1	124/1	334/1	340/1	503/1
SiO_2	65.25	69.42	67.08	72.08	68.56	71.38
TiO_2	0.79	0.56	0.80	0.42	0.49	0.54
Al_2O_3	14.18	14.95	15.95	13.88	15.64	14.08
FeO	6.42	3.90	5.03	3.36	3.89	4.59
MnO	0.18	0.11	0.12	0.08	0.09	0.15
MgO	2.28	1.66	1.66	1.26	1.60	1.79
CaO	6.81	2.72	2.59	3.24	4.06	1.72
Na_2O	3.42	5.37	4.83	4.17	3.83	4.65
K_2O	0.43	1.16	1.71	1.35	1.66	0.93
P_2O_5	0.24	0.17	0.23	0.16	0.18	0.18
Total	100.00	100.02	100.00	100.00	100.00	100.01
LOI	2.25	2.50	2.00	2.05	3.30	1.85
Ni	51	18	12	23	16	19
Cu	29	7	9	12	9	20
Zn	74	51	68	48	55	68
Ga	16	13	11	14	12	13
Rb	14	22	40	31	37	22
Sr	753	242	325	318	378	207
Y	26	22	23	22	16	18
Zr	133	150	169	133	143	121
La		18		23		24
Ce		32		41		43
Nd		18		23		23
Sm		3.6		4.5		4.8
Eu		1.2		1.3		1.3
Gd		3.2		3.3		3.6
Er		1.7		1.7		2.0
Yb		1.5		1.4		1.7

Major elements determined by XRF at the United Institute of Geology, Geophysics and Mineralogy (Novosibirsk), trace elements by X-ray fluorescence spectrometry at the Institute of Lithosphere (Moscow), rare earth elements by ion-coupled plasma at the same Institute. Oxides in wt% (recalculated to make 100% total), trace elements in ppm. Sample numbers correspond to site numbers in Figure 4. LOI, loss-on-ignition.

Table 3 Sm-Nd isotopic data for volcaniclastic rocks

Sample	Age (Ma)	Nd (ppm)	Sm (ppm)	$^{147}Sm/^{144}Nd$	$^{143}Nd/^{144}Nd$	$\varepsilon_{Nd(t)}$	$T_{(DM)}$ (Ma)
291/1	700	16.57	3.22	0.1162	0.512172 ± 4	–1.9	1529
503/1	700	20.9	4.00	0.1147	0.512087 ± 6	–3.4	1636

The analysis was made by V. Kovach at the Institute of Precambrian Geology and Geochronology (St. Petersburg).

traced along the inner part of the Oka Belt (Dobretsov *et al.* 1988; Sklyarov & Medvedev 1988; Sklyarov & Postnikov 1990; Sklyarov *et al.* 1996). It comprises the greenschist facies rocks, mainly metabasites, which show occasional relics of HP–LT minerals. Such rocks were found in almost all the studied areas (numbers 2–5, Fig. 2). Most of the zone is composed of actinolite-chlorite-epidote-albite greenschists, formed after basalts and gabbro, and some phengite-chlorite-quartz-albite schists. The HP–LT rocks generally show distinct schistosity and metamorphic banding expressed by alteration of 0.5–3 mm-thick 'layers' composed of epidote, amphibole or albite. Winchite is a common mineral. The Na_2O content is up to 4.5% in the core and decreases to the rim. Crossite was found as rare relics fringed with winchite or actinolite. The Na_2O content reaches 5.6% in the core and decreases to the rim. White micas are characterized by high contents of celadonite component (Si = 3.3–3.4 pfu) both in metabasitic and in the associated metapelitic schists.

The fact that crossite was found only in rocks of most favorable chemical composition, as well as absence of lawsonite and glaucophane, permits to tentatively estimate the metamorphic conditions as intermediate between the proper glaucophane-schist and greenschist facies with the pressure ranging approximately from 5 to 7 kbar. The temperature of metamorphism equaled 380–450°C judging by mineral associations and absence of stilpnomelane.

THOLEIITIC INTRUSIONS

The northern segment of the Oka Belt is intruded by basaltic magma and contains numerous diabase and gabbro-diabase bodies. In the upper courses of the Jakhoshop and Dayalyk Rivers, such intrusions are mostly sills of several meters to several dozens of meters thick (Fig. 4). In this area, intrusive bodies are the least deformed and altered and sometimes preserve initial intrusive contacts with the Oka Group shales and volcaniclastic rocks. In this area, one can undoubtedly distinguish massive intrusions and basalts which have turned into greenschists. Southwards the deformation of intrusions increases and on the Tustuk River banks their marginal parts become schistose yet display evident difference from oceanic metabasalts. On the ridge between the Tustuk and Oka Rivers some diabase bodies have completely changed into greenschists and some grenschist lenses can hardly be distinguished from metabasaltic ones. This was a result of exhumation processes. The most modified intrusions are presumably contained in the Kharatologoy metamorphic complex where they turned into amphibolites.

In the northern area, sills are composed of saussuritized plagioclase, clinopyroxene and some olivine, replaced by chlorite. Sometimes, the intrusions are differentiated up to trondhjemite lithology. Chemical composition is variable because of magma differentiation (Table 4). Variation diagrams (not shown) show distinct tholeiitic trend: FeO* and TiO_2 are steadily increasing, whereas MgO is decreasing from 10 to approximately 4 or 3%. At this point, mass crystallization of apatite and Fe oxides begins. Acidic end-members are strongly enriched with rare earth elements (REE), Zr and some other 'incompatible' elements. Differentiation affects the bulk concentration of REE, but has minor effect on the REE pattern (Fig. 8). The latter shows depletion in light REE, which is typical of normal MORB magma, originated from a depleted mantle source. The Nd isotopic composition confirms this conclusion. The Sm-Nd mineral isochron for gabbro-diabase 519/1 indicates the age of crystallization of 736 ± 43 Ma and εNd(T) as high as $+7.8 \pm 0.5$ indicating a strongly depleted mantle source (Table 5, Fig. 9).

The Oka intrusive rocks show some enrichment with large ion lithophile elements (LILE) and minor negative Nb anomalies. We might suggest that these features were a result of contamination of MORB-like magma with the prism sediments.

THE OKA PRISM AGE

The only way to determine the age of the Oka accretionary prism is to date the igneous bodies that intrude it. The Sm-Nd isotopic age, based on gabbro minerals, has been reported above. The isochron parameters were not very good, so we had to obtain a more reliable zircon U-Pb age. We have dated the trondhjemite sample 521/2, an acidic member of the above tholeiitic suite. The discordia is based on three zircon grain-size fractions (Table 6). Analytical points were grouped near the upper intersection with concordia that occur at the point 753 ± 16 Ma (Fig. 10). These results confirm the Sm-Nd age of the sills within the confidence interval.

The data indicate the upper age limit for the Oka Group host rocks. We can suggest that the host

Table 4 Chemical composition for tholeiitic intrusions in the northern Oka Belt

	119/2	394/1	401/1	401/2	519/1	521/2	521/3	317/1
SiO_2	50.61	44.79	48.99	52.23	47.52	75.94	61.84	50.47
TiO_2	1.66	2.74	3.25	1.36	0.75	0.21	0.72	0.97
Al_2O_3	15.23	11.91	10.95	12.45	14.28	11.24	12.70	16.31
FeO	12.72	17.62	17.97	16.58	8.91	3.12	11.10	8.58
MnO	0.23	0.25	0.32	0.32	0.16	0.07	0.24	0.17
MgO	6.63	5.69	3.90	1.70	9.49	0.53	1.25	7.43
CaO	8.39	11.46	6.02	5.80	14.13	0.41	2.66	12.40
Na_2O	4.37	1.30	3.77	3.15	1.66	5.58	5.77	3.10
K_2O	0.04	0.34	0.44	0.47	0.10	0.79	0.40	0.49
P_2O_5	0.13	0.17	0.27	0.63	0.11	0.09	0.17	0.09
LOI	3.05	3.60	2.90	4.20	2.80	0.85	1.90	3.50
Total	100.01	99.87	98.78	98.89	99.91	98.83	98.75	100.01
V	373		195		289		35	244
Cr	153		3		1110		14	807
Ni	74		3		161		7	114
Rb	0.81		9.79		1.16		7.23	12.13
Sr	211		82		212		202	299
Y	45		76		24		181	31
Zr	100		114		39		267	60
Nb	2.13		3.19		0.94		14.91	1.75
Ba	126		61		17		180	68
La	3.54		4.5		1.19		16.28	2.3
Ce	10.72		14.97		3.89		48.72	7.23
Pr	1.77		2.6		0.72		8.08	1.19
Nd	9.85		14.71		4.36		44.62	6.92
Sm	3.44		5.4		1.72		15.27	2.48
Eu	1.15		1.98		0.72		4.9	0.96
Gd	4.9		8.1		2.7		22.3	3.6
Tb	0.87		1.44		0.46		3.82	0.61
Dy	6.22		10.48		3.41		27.89	4.31
Ho	1.59		2.66		0.81		6.95	1.06
Er	4.12		6.69		2.24		18.88	2.74
Tm	0.61		1.03		0.34		3.04	0.43
Yb	3.9		6.36		2.14		20.12	2.75
Lu	0.58		0.96		0.31		3.18	0.38

Major elements analysis was made by X-ray fluorescence spectrometry technique, United Institute of Geology, Geophysics and Mineralogy, Novosibirsk. Rare-earth and trace elements by ICP-MS at the Institute of Mineralogy, Geochemistry and Crystal Chemistry of Rare Elements, Moscow. Blank spaces denote no data. Oxides in percentage, trace elements in ppm. Sample numbers correspond to site numbers in Figure 4. LOI, loss-on-ignition.

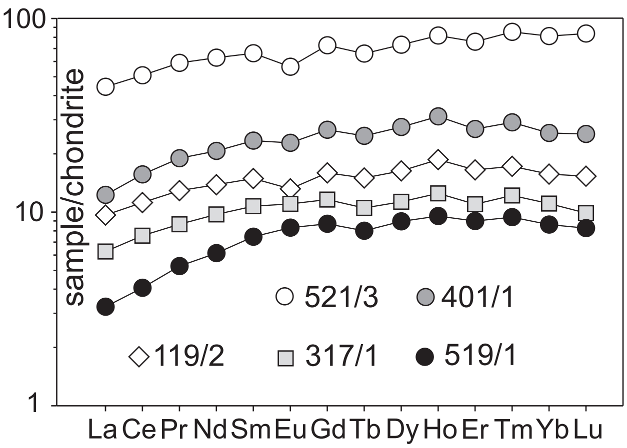

Fig. 8 Rare earth elements patterns for the Yakhoshop and Dayalyk Rivers igneous rocks.

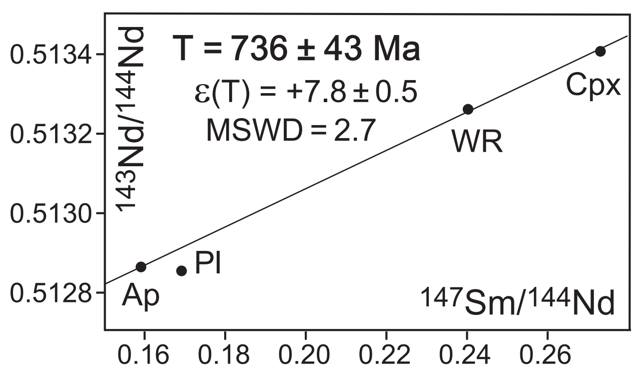

Fig. 9 Sm-Nd isotopic diagram for sample 519/1–04. Isochron and initial Nd compositions are calculated by three points (except saussuritized plagioclase). The 2σ intervals are indicated. Ap, apatite; Cpx, clinopyroxene; Pl, plagioclase; WR, whole rock.

Table 5 Sm-Nd isotopic data for the gabbro-diabase 519/1 minerals and whole rock

	Nd (ppm)	Sm (ppm)	^{147}Sm/ ^{143}Nd	^{144}Nd/ ^{144}Nd
Whole rock (WR)	4.092	1.620	0.2393	0.513255 ± 10
Plagioclase (Pl)	3.098	0.866	0.1690	0.512853 ± 7
Clinopyroxene (Cpx)	5.926	2.673	0.2727	0.513400 ± 9
Apatite (Ap)	401.3	105.9	0.1595	0.512858 ± 7

The isotopic measurements were carried out on a MAT 262 mass spectrometer in a static mode. The ^{143}Nd/^{144}Nd ratios are normalized to ^{146}Nd/^{144}Nd = 0.7219. The external precision of the ^{143}Nd/^{144}Nd ratios has been determined with La Jolla Nd standard yielding 0.511842 ± 14 (n = 17). Error for ^{147}Sm/^{144}Nd ~0.2% (2 σ) and for element concentrations – 1%.

Table 6 The U-Pb isotopic data for zircons for sample 521/2

Fraction (μm)	Weight (g)	U (ppm)	Pb (ppm)	^{206}Pb/^{204}Pb	^{206}Pb/^{207}Pb	^{206}Pb/^{208}Pb	^{206}Pb/^{238}U	^{207}Pb/^{235}U	^{207}Pb/^{206}Pb
+75	0.0021	149.22	18.83	882	12.653	3.116	0.1037 (636.0 Ma)	0.8969 (650.1 Ma)	699.1 ± 17 Ma
+60–75	0.0021	124.33	17.89	282	8.7812	2.5696	0.1054 (646.1 Ma)	0/9128 (658.6 Ma)	701.5 ± 19 Ma
–60, SD	0.0015	126.14	18.403	1860	13.879	3.2626	0.1234 (750.2 Ma)	1.0954 (751.1 Ma)	753.8 ± 9.1 Ma

Zircons were isotopically studied by the Krogh (1973) method. The U and Pb concentrations were determined by isotopic dilution using the mixed spike 208Pb + 235 U. The lead blank was 0.1 ng. Isotopic composition was estimated with mass spectrometer TSN 206 A, Cameka Co. Isotopic ages were calculated using the Ludwig program (1991). Errors in the U-Pb ratios made up 0.5%. The common lead correction was introduced according to Stacey and Kramers (1975) model for 700 Ma.

sediments are not much older and are also Late Neoproterozoic. Most of igneous bodies are shallow-level intrusions. Curved contacts of some of them indicate that they intruded into poorly lithified sediments.

The obtained age roughly corresponds to the Rb-Sr age of volcanic rocks in the adjacent Sarkhoi Continental Arc: 718 ± 30 Ma (Buyakaite *et al.* 1989). Consequently, the Oka prism and the Sarkhoi Arc are thought to have existed simultaneously and acted as two members of the same geodynamic system. This system can operate up to Late Baikalian orogeny, which occurred at approximately 600 Ma (Kuzmichev *et al.* 2005). We do not know what happened in the interval of 150 my between 753 ± 16 and 600 Ma and how long the Oka prism remained active. The answer can hardly be obtained by studying the Oka prism. Further dating of the Sarkhoi volcanics can yield the age of suprasubduction volcanism and convergence duration, although the accretionary subduction could be changed into the erosional one.

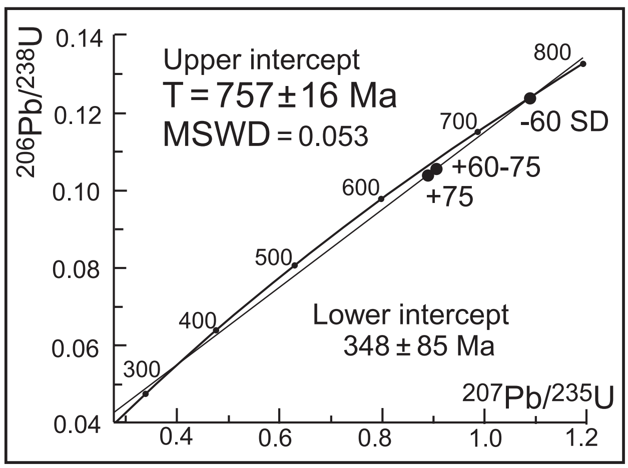

Fig. 10 The U-Pb diagram for sample 521/2.

DISCUSSION

All the information on the Oka Belt structure and composition has been furnished above to bring a reader to the idea that it can be interpreted as a Neoproterozoic accretionary prism. We shall now ground this interpretation by discussing the above data in the context of accretionary processes and by comparing the Oka Belt with accretionary prisms whose origin is confidently known.

STRUCTURE

Structural studies of recent and Mesozoic accretionary complexes have shown at least two main distinctive deformation stages. The first stage is a layer-parallel extension as a result of rapid rock accumulation, piling and underthrusting beneath the accretionary wedge resulting in boudinage, flattening and foliation. The second stage is a wedge shortening, resulting in the seaward thrusting and imbrication accompanied by slaty cleavage (e.g. Fisher & Byrne 1987; Sample & Moore 1987; Taira *et al*. 1992a,b; Hashimoto & Kimura 1999). As shown above, the Oka Belt shows the same succession as in the reference prisms.

Sample and Moore (1987) noted that above structural features can not be attributed solely to accretionary wedges, but might be expected for any type of thrust belts. A similar imbricated structure is known to have resulted from collision instead of sediment accretion (e.g. Alavi 2004). Moreover, there is a viewpoint that a distinctive Shimanto Belt structure has originated from collision (Stein *et al*. 1994). However, regarding our particular Late Neoproterozoic case we can prove that no other thrust belt is likely to exhibit the same structural features. On both sides of the Oka Belt there are terrains that include similar lithologies but show a different structure. At the basement of the Sarkhoi volcanics there lies the Dunzhugur ophiolite overlain by a thick coherent turbidite sequence deposited in the forearc basin (Kuzmichev 2004). The sequence preserves all primary sedimentary textures and does not show any structural features inherent to the Oka Belt rocks except the slaty cleavage in the upper portion. On the other side, there lies the Shishkhid ophiolite overlain by Kharaberin Formation including turbidite and mudstone deposits accumulated in the back-arc setting (Kuzmichev *et al*. 2005). These sediments, although folded, were substantially less deformed than the Oka Belt. Despite overall great compression strain as a result of collision episodes, both Neoproterozoic terrains adjacent to the Oka Belt do not show any imbrication. The rocks show neither early stage extension nor boudinage.

The Late Neoproterozoic structure of all the three terrains was overprinted by two events of imposed deformation at the end of Vendian and the beginning of Ordovician (Kuzmichev 2004). Moreover, the Dunzhugur unit experienced one more orogeny in the Mid-Neoproterozoic time. This means that the superposed collision events were not responsible for structural features specific for the Oka Belt. It certainly preserved the structural style, differing significantly from the surrounding terrains. We believe that this distinction was inherited from the accretionary stage of the prism formation.

The Oka Thrust Belt presently shows a predominantly landward vergence, opposite to what could be expected in an accretionary complex. As indicated in the structural chapter, some examples really prove that in the Neoproterozoic time the vergence was faced seaward. We refer the rotation of thrust planes to the effect of imposed deformations. These processes do not imply any significant rotation because the recent thrust planes in the Oka prism dip at the angle of 70–85° on average. Moreover, in some places (e.g. the Hugein River banks) the Oka Belt lower portion preserved the seaward vergence, which is discordant to the sole thrust.

LITHOLOGY

Like most accretionary wedges the Oka Belt is predominantly composed of greywacke turbidite deposits, which might represent the trench sedimentation. Our data are, however, insufficient to confidently define the depositional setting. Besides these common deposits, the Oka Group contains volcaniclastic rocks. Similar rocks are known, however, in the Nankai prism and in the Miocene portion of the Shimanto Belt, which contain volcaniclastic conglomerates with rounded or sometimes angular porphyry debris and ash layers (Charvet *et al*. 1990; Taira *et al*. 1992a; Underwood *et al*. 2003).

A carbonate olistostrome is another atypical rock type, which indicates a carbonate shoal upslope. A similar olistostrome was described in the Shimanto Belt, in the lower part of terrigenous complex filling a foredeep superposed on the accretionary prism. Up the section, the olistostrome is replaced by shales of basinal sedimentation, which, higher up, are covered by cross-stratified shorefacing sandstone (Taira *et al*. 1988, 1992a). Although we have not encountered any distinct shallow-water deposits in the Oka Belt, many factors indicate that the olistostrome and, possibly, the overlying rocks are positioned similarly as in the Shimanto Belt and can be interpreted as superimposed strata. Hibbard and Karig (1990b) noted that initiation of shallow-marine basin atop the Shimanto accretionary prism was related to Shikoku Ridge subduction and possibly reflected the topographic change in the subducting plate. The forearc uplift caused by ridge subduction was also proposed by Osozawa (1997). The same can also be suggested to the Oka olistostrome, located in the northern belt segment that experienced the similar ridge subduction event.

OCEANIC ROCKS

Oceanic sediments and mid-ocean ridge basalts are the most notable feature of the well-studied Shimanto accretionary prism, which enables to understand its origin (Taira *et al.* 1992a). Pillow-basalt, basaltic tuff, radiolarian chert, red claystone and nannoplankton limestone occur in the form of blocks or tectonic slivers in mélange zones and represent the uppermost subducted oceanic crust (Taira *et al.* 1988, 1992a; Kimura & Mukai 1991, 1995).

Altered MORB-like basalts are common in the Oka Belt. They can be united with the associated gabbro and serpentinite into the ophiolite complex representing the oceanic lithosphere. This association is rare on the Earth where great majority of ophiolites are of suprasubduction type (Shervais 2001). Usually oceanic rocks are completely subducted but they can be efficiently trapped in accretionary complexes. Pelagic oceanic sediments so common for Mesozoic accretionary complexes cannot be confidently identified in Neoproterozoic belts because of the absence of planktonic rock-forming organisms. However, some analogs represented by thin-laminated red argillite and jasper are seen in the Oka Belt.

The ocean floor basalts chiefly occur in the inner part of the Oka Belt. This is typical of accretionary prisms, where underplated material from deeper horizons of the prism body was exhumed. This is also true for HP–LT metamorphic rocks (e.g. Platt 1986).

BLUESCHISTS

The discovery of blueshists in the Oka Belt is a strong argument in favor of its accretionary prism origin. The blueschists in fold belts come up from a subduction zone and are an essential attribute of the accretionary prism setting. The HP–LT metamorphics have been reported for many fossil accretionary prisms (Wakabayashi & Unruh 1995; Kimura *et al.* 1996; Tagami & Hasebe 1999; Wallis *et al.* 2001; others). In most cases, they are associated with the oceanic mafic rocks occurring in the mélange.

THOLEIITIC INTRUSIONS

The accretion prism environment is usually amagmatic and the Oka Belt tholeiitic intrusions need to be explained. However, similar occurrences of intrusive rocks are known in the Oligocene and Miocene portions of the Shimanto Belt: numerous diabase dikes and sills crop out on the southern capes of Shikoku Island and Kii Peninsula. Large bodies are composed of gabbo-diabases and gabbro-diorites. Some of them were differentiated and show granophyric composition as most evolved members similarly to the Oka Belt. The Shimanto diabase and gabbro are geochemically alike the Shikoku Basin basalts, and magmatism is explained by the Shikoku spreading ridge arrival into the subduction zone (Miyake 1985; Hibbard & Karig 1990a; Taira *et al.* 1992a; Kimura *et al.* 2005). Such mode of the oceanic ridge subduction is not unique (e.g. Forsythe *et al.* 1986; Osozawa 1992; Maeda & Kagami 1996).

We believe that mafic igneous bodies in the Oka accretionary prism are of the same origin as in the Shimanto Belt. In Late Neoproterozoic time, an oceanic spreading center invaded beneath the Oka accretionary prism and produced the normal MORB-like melts. The magma differentiation and its contamination by the prism sediments were responsible for the igneous composition discussed above. Such intrusions occur only in the Oka Belt northern limb, which can indicate orthogonal position of oceanic ridge to convergent margin, just like Shikoku Ridge.

THE NEOPROTEROZOIC TECTONIC SETTING OF THE OKA BELT

A final argument to prove the accretionary origin of the Oka belt is its presumed Neoproterozoic tectonic position in front of the Sarkhoi Continental Arc (see figure 15 of Kuzmichev *et al.* 2005). This was somewhat like the position of the Shimanto-Nankai accretionary wedge in front of the Japanese Arc. On the opposite side of the Oka prism there was the Paleoasian Ocean whose closest tectonic feature that we know was the Shishkhid Island Arc. The latter lacked the continental basement and its rear part was oriented to the Oka prism.

CONCLUSIONS

The Neoproterozoic Oka Belt composed of turbiditic clastic rocks reveals distinct structural and compositional features that allow to interpret it as a fossil accretionary prism. These are: (i) imbricated structure with a presumably seaward vergence; (ii) slivers of oceanic basalts of MORB and OIB geochemical affinities incorporated into the prism body; and (iii) mélange with blueschist slivers. The Hugein area oceanic abyssal tholeiites and OIB trapped in the prism body deserve special study because these rocks are the only direct evidence indicating the existence of Paleoasian Ocean in Neoproterozoic time that permit to probe its lithosphere.

Besides the above features typical of accretionary prism, the northern Oka Belt shows some uncommon features including tholeiitic intrusions, volcaniclastic material and a marked carbonate olistostrome. All these features are also inherent to the northern Shimanto Belt in the Shikoku Island and Kii Peninsula. It is quite possible that they all were the effect of the oceanic ridge subduction (e.g. Hibbard & Karig 1990b). The same episode in the Oka prism life history dates back to 753 ± 16 Ma. The amazing similarity of Late Neoproterozoic and Miocene situations of the orthogonal ridge subduction is very promising for studies of the accompanying phenomena in the northern Oka Belt.

The Oka prism accretion followed the initiation of subduction beneath the Sarkhoi continental margin. This event was caused by Early Baikalian orogeny, which happened at 800 Ma (Kuzmichev *et al*. 2001). The prism was piling up in front of the Sarkhoi Continental Arc through the second half of Neoproterozoic time although its exact lifetime interval is unknown. The next dated event, which confines the prism history was its collision with the Shishkhid Oceanic Arc, which occurred at approximately 600 Ma (Kuzmichev *et al*. 2005).

The sediment accumulation and underplating in accretionary wedges are one of the major geodynamical mechanisms operating at convergent margins, which result in lateral growth of continental crust. However, due to the process, the continent's own material is mainly returned back. A huge bulk of sialic material has been accumulated by the Oka prism. This shows that the mechanism was as intensive in the Neoproterozoic time as it was in the Cenozoic one. The size of the Oka Belt is comparable with the adjacent arc terrains even in its recent, tightly compressed structure (Fig. 2).

The Oka Belt is the largest Neoproterozoic accretionary prism known to the authors. It is possibly the only example of a well-preserved Precambrian accretionary prism and therefore requires further detailed systematic structural, sedimentological and petrological studies.

ACKNOWLEDGEMENTS

We greatly appreciate the work of reviewers, Prof Shoichi Kiyokawa and especially Prof Soichi Osozawa, whose extensive review was quite useful and prevented us from erroneous interpretation. We are also grateful to Prof Asahiko Taira whose kind advice was of great help. We are deeply obliged to Prof Akira Ishiwatari for the final editing of the manuscript which greatly improved its style and contents. The research was supported by the Russian Academy of Sciences (Program 'Central Asian fold belt: geodynamics and main stages of continental crust formation').

REFERENCES

AKTANOV V. I. & SKLYAROV E. V. 1990. Geology and metamorphism of Kharatologoy block (East Sayan). *Russian Geology and Geophysics* **31**, 82–9.

ALAVI M. 2004. Regional stratigraphy of the Zagros fold-thrust belt of Iran and its proforeland evolution. *American Journal of Science* **304**, 1–20.

ARSENTIEV V. P. & VOLKOLAKOV F. K. 1964. Proterozoic and Cambrian deposits of East Sayan. *In The USSR Geology*, Vol. XXXV *Buriatskaya ASSR*, Part 1, pp. 69–88, 135–147, Nedra, Moscow (in Russian).

BELICHENKO V. G., BOOS R. G., DOBRETSOV N. L., SKLYAROV E. V. & POSTNIKOV A. A. 1989. Tectonics and problems of tectonic evolution of southeast East Sayan. *In* Dobretsov N. L. & Ignatovich V. I. (eds). *Geology and Ore Potential of East Sayan*, pp. 4–21. Nauka, Novosibirsk (in Russian).

BUYAKAITE M. I., KUZMICHEV A. B. & SOKOLOV D. D. 1989. The 718 Ma – Rb-Sr errorchron of the Sarkhoi suite (East Sayan). *Transactions (Doklady) of Russian Academy of Sciences* **309**, 150–4 (in Russian).

CHARVET J., FAURE M., FABBRI O., CLUZEL D. & LAPIERRE H. 1990. Accretion and collision during East-Asiatic margin building – a new insight on the peri-Pacific orogenies. *In* Wiley T. J., Howell D. C. & Wong F. L. (eds). *Terrain Analysis of China and the Pacific Rim. Circum-Pacific Council for Energy and Mineral Resources. Earth Science Series*, Vol. 13, pp. 161–91. Houston, Texas.

DOBRETSOV N. L., KARSAKOV E. V. & SKLYAROV E. V. 1988. Glaucophane-schist belts in the southern Siberia and Gis-Amur region. *Russian Geology and Geophysics* **29**, 3–11.

DODIN A. L., GURJANOVA V. N., MAN'KOVSKY V. K., RESHETOVA S. A., SEMEINAYA B. G. & GOL'MAN E. I. 1971. *The Oka and Iya Stratigraphic Sections of Late Precambrian of East Sayan*. Nedra, Moscow.

DONSKAYA T. V., SKLYAROV E. V., GLADKOCHUB D. P., MAZUKABZOV A. M. & VASIL'EV E. P. 2004. The

Shutkhulay metamorphic complex, Southeastern Sayan: Specific features of metamorphism and a model of formation. *Russian Geology and Geophysics* **45**, 175–92.

FISHER D. & BYRNE T. 1987. Structural evolution of underthrusted sediments, Kodiak Island, Alaska. *Tectonics* **6**, 775–9.

FORSYTHE R. D., NELSON E. P., CARR M. J. *et al.* 1986. Pliocene near-trench magmatism in southern Chile: A possible manifestation of ridge collision. *Geology* **14**, 23–7.

HASHIMOTO Y. & KIMURA G. 1999. Underplating process from mélange formation to duplexing: Example from the Cretaceous Shimanto belt, Kii Peninsula, southwest Japan. *Tectonics* **18**, 92–107.

HIBBARD J. P. & KARIG D. E. 1990a. Structural and magmatic responses to spreading ridge subduction: An example from southwest Japan. *Tectonics* **9**, 207–30.

HIBBARD J. P. & KARIG D. E. 1990b. Alternative plate model for Early Miocene evolution of the southwest Japan margin. *Geology* **18**, 170–4.

KATYUKHA YU. P. & ROGACHEV A. M. 1983. On the age of Mangatgol, Dabanzhalga and Oka series of East Sayan. *Russian Geology and Geophysics* **24**, 68–78.

KIMURA G. & LUDDEN J. 1995. Peeling oceanic crust in subduction zones. *Geology* **23**, 217–20.

KIMURA G. & MUKAI A. 1991. Underplated units in an accretionary complex: Mélange of the Shimanto belt of Eastern Shikoku, Southwest Japan. *Tectonics* **10**, 31–50.

KIMURA G., MARUYAMA S., ISOZAKI Y. & TERABAYASHI M. 1996. Well-preserved underplating structure of the jadeitized Franciscan complex, Pacheco Pass, California. *Geology* **24**, 31–50.

KIMURA J.-I., STERN R. J. & YOSHIDA T. 2005. Reinitiation of subduction and magmatic responses in SW Japan during Neogene time. *Geological Society of America Bulletin* **117**, 969–86.

KROGH T. 1973. A low contamination method for hydrothermal decomposition of zircon and extraction of U and Pb for isotopic age determination. *Geochimica et Cosmochimica Acta* **37**, 485–94.

KUZMICHEV A. B. 1997. Structure of Upper Riphean Oka series on the right bank of the Tustuk River (East Sayan). *Geology and Prospecting* **3**, 21–36 (in Russian).

KUZMICHEV A. B. 2004. *Tectonic History of the Tuva-Mongolian Massif: Early Baikalian, Late Baikalian and Early Caledonian stages.* Probel, Moscow (in Russian).

KUZMICHEV A. B., BIBIKOVA E. V. & ZHURAVLEV D. Z. 2001. Neoproterozoic (800 Ma) orogeny in the Tuva-Mongolian Massif (Siberia): Island arc – continent collision at the northeast Rodinia margin. *Precambrian Research* **110**, 109–26.

KUZMICHEV A., KRONER A., HEGNER E., DUNYI L. & YUSHENG W. 2005. The Shishkhid ophiolite, northern Mongolia: A key to the reconstruction of a Neoproterozoic island-arc system in central Asia. *Precambrian Research* **138**, 125–50.

LUDWIG K. B. 1991. ISOPLOT program. *USA Geol.* Survey Open-File Report 91.

MAEDA J. & KAGAMI H. 1996. Interaction of a spreading ridge and an accretionary prism: Implications from MORB magmatism in the Hidaka magmatic zone, Hokkaido, Japan. *Geology* **24**, 31–4.

MIYAKE Y. 1985. MORB-like tholeiites formed within the Miocene forearc basin, Southwest Japan. *Lithos* **18**, 23–34.

OSOZAWA S. 1992. Double ridge subduction recorded in the Shimanto accretionary complex, Japan, and plate reconstruction. *Geology* **20**, 939–42.

OSOZAWA S. 1997. The cessation of igneous activity and uplift when actively spreading ridge is subducted beneath an island arc. *Island Arc* **6**, 361–71.

PLATT J. P. 1986. Dynamics of orogenic wedges and uplift of high-pressure metamorphic rocks. *Geological Society of America Bulletin* **97**, 1037–10.

POSTNIKOV A. A. & SKLYAROV E. V. 1988. The Oka series. *In* Dobretsov N. L. & Ignatovich V. I. (eds). *Geology and Metamorphism of East Sayan*, pp. 52–7, Nauka, Novosibirsk (in Russian).

RAMSEY J. G. & HUBER M. I. 1987. *The Techniques of Modern Structural Geology*, Vol. 2*: Folds and Fractures.* Academic Press, Oxford.

ROSCHEKTAEV P. A., KATYUKHA Y.P. & ROGACHEV A. M. 1983. Main stratigraphic features of southeast East Sayan. *In* Khomentovsky V. V. (ed.). *Stratigraphy of Late Precambrian and Early Palaeozoic. Southern Fringing of Siberian Platform*, pp. 19–43. Institute of Geology and Geophysics, Novosibirsk (in Russian).

SAMPLE J. C. & MOORE J. C. 1987. Structural style and kinematics of an underplated slate belt, Kodiak and ajacent islands, Alaska. *Geological Society of America Bulletin* **99**, 7–20.

SHERVAIS J. W. 2001. Birth, death and resurrection: The life cycle of suprasubduction zone ophiolites. *Geochemistry Geophysics Geosystems* **2**, paper number 2000GC000080, 45 p.

SKLYAROV E. V. & MEDVEDEV V. N. 1988. High-pressure metamorphism. *In* Dobretsov N. L. & Ignatovich V. I. (eds). *Geology and Metamorphism of East Sayan*, pp. 126–8. Nauka, Novosibirsk (in Russian).

SKLYAROV E. V. & POSTNIKOV A. A. 1990. The Khugein high-pressure belt of Northern Mongolia. *The Transactions (Doklady) of the Russian Academy of Sciences* **315**, 950–4.

SKLYAROV E. V., POSTNIKOV A. A. & POSOKHOV V. F. 1996. Structural setting, metamorphism and petrology of the Hugein Group (Northern Mongolia). *Russian Geology and Geophysics* **37**, 69–78.

STACEY J. S. & KRAMERS J. D. 1975. Approximation of terrestrial lead isotope evolution by a two-stage model. *Earth and Planetary Science Letters* **26**, 207–21.

Stein G., Charvet J., Lapierre H. & Fabbri O. 1994. Geodynamic setting of volcano-plutonic rocks in so-called paleo-accretionary prisms – fore-arc activity or post-collisional magmatism – the Shimanto belt as a case study. *Lithos* **33**, 85–107.

Tagami T. & Hasebe N. 1999. Cordilleran-type orogeny and episodic growth of continents: Insights from the circum-Pacific continental margins. *Island Arc* **8**, 206–17.

Taira A., Katto J., Masayuki T., Okamura M. & Kodama K. 1988. The Shimanto belt in Shikoku, Japan – evolution of Cretaceous to Miocene accretionary prism. *Modern Geology* **12**, 5–46.

Taira A., Byrne T. & Ashi J. 1992a. *Photographic Atlas of An Accretionary Prism. Geologic Structures of the Shimanto Belt, Japan*. Springer-Verlag, Tokyo.

Taira A., Hill I., Firth J. *et al.* 1992b. Sediment deformation and hydrogeology of the Nankai Trough accretionary prism: Synthesis of shipboard results of ODP Leg 131. *Earth and Planetary Science Letters* **109**, 431–50.

Underwood M. B., Moore G. F., Taira A. *et al.* 2003. Sedimentary and tectonic evolution of a trench-slope basin in the Nankai subduction zone of Southwest Japan. *Journal of Sedimentary Research* **73**, 589–602.

Wakabayashi J. & Unruh J. 1995. Tectonic wedging, blueschist metamorphism, and exposure of blueschists: Are they compatible? *Geology* **23**, 85–8.

Wallis S., Takasu A., Enami M. & Tsujimori T. 2001. Eclogite and Related Metamorphism in the Sanbagawa Belt, Southwest Japan. *Bulletin of Research Institute of Natural Science, Okayama University of Science* **26**, 3–19.